PHYSICAL REVIEW B VOLUME 52, NUMBER 9 1 SEPTEMBER 1995-I

Stresses in strained GeSi stripes: Calculation and determination from Raman measurements

S. C. Jain*
Clarendon Laboratory, Oxford OX1 3PU, United Kingdom

B. Dietrich and H. Richter
Institute of Semiconductor Physics, Frankfurt/Oder, Germany

A. Atkinson and A. H. Harker
AEA Technology, Harwell Oxon OX11 0RA, United Kingdom
(Received 3 February 1995)

Three mechanisms by which edges induce stress relaxation in GeSi strained stripes are described and their relative importance is discussed. Relaxation of stresses in the middle of the layers with l/h(=half-width/thickness) varying from 3 to 100 is calculated including the effect of the two mechanisms which are important in this range. The values calculated in this manner agree with our recent finite element calculations. Since the stresses in the stripes in the two orthogonal directions are not equal and since the stripes are usually grown in the [110] direction on a (100) substrate, determination of stress and strain using Raman measurements is not straightforward. A relation between the shifts $\Delta\omega_3$ in the LO Raman frequency and stresses and strains in the stripe is established. With the help of this relation, a single measurement of $\Delta\omega_3$ is sufficient to determine all the stresses and strains in the middle of the top layer of the stripe. Using recently measured values of $\Delta\omega_3$ and known values of phonon deformation potentials, stresses in $Ge_{0.14}Si_{0.86}$ stripes are determined. The values determined in this manner agree with the calculated values within the uncertainty in the available values of deformation potentials. The method developed is general and can be used for other semiconductor stripes irrespective of whether the strain is thermal or due to lattice mismatch.

I. INTRODUCTION

GeSi strained layers are of great importance for designing and fabricating new devices and enhancing the performance of existing devices.[1] Recently several authors have studied theoretically[2-8] and experimentally[9-12] stresses in narrow long stripes (see Fig. 1). The structures investigated include GaAs on Si,[5] InP on Si,[12] InGaAs on GaAs,[9] and GeSi stripes on Si.[10] We show in this paper that approximations made in the theoretical papers[2-8] give large errors in the values of stresses in *narrow* stripes and calculate more accurate values. Experimental studies of the stripes have been made using Raman and electroluminescence (EL) measurements. Since the stresses in the stripe coordinate σ'_{xx} and σ'_{yy} are not equal, it was not possible to determine accurately stresses (or strains) using these measurements. Reliable theoretical or experimental values of the edge-induced stresses in the stripes are not available. In this paper we calculate and determine from the existing Raman measurements the stresses (and strains) in GeSi stripes.

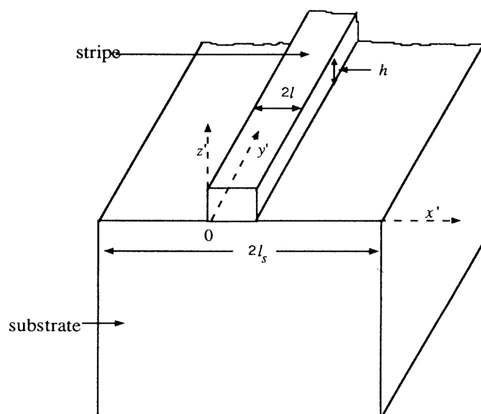

FIG. 1. Schematic diagram of a stripe grown on a Si substrate.

The paper is divided into five sections. The theory of edge-induced stress relaxation is discussed in Sec. II. The three mechanisms by which the edges relax stresses in the stripes are discussed and their relative importance is described. The values of σ'_{xx}/σ_0 (σ_0 is the stress in an infinitely wide stripe) at the midline of the stripes are also calculated for different values of l/h in this section. A relation between the shift $\Delta\omega_3$ and stresses (and strains) in the top layer of the stripe is established in Sec. III. A method to determine stress and strain in the stripes using this relation and Raman measurements is described. Using this relation and values of $\Delta\omega_3$ measured by Dietrich *et al.*,[10] experimental values of σ'_{xx}/σ_0 are determined and compared with the calculated values in Sec. IV. A summary of important results and concluding remarks is given in Sec. V.

0163-1829/95/52(9)/6247(7)/$06.00 ©1995 The American Physical Society

II. THEORY OF EDGE-INDUCED STRESS RELAXATION IN NARROW STRIPES

For convenience of discussion we consider a layer under compression, though the arguments given here also apply to layers under tension. The two edges of a narrow strained stripe induce strain relaxation by three different mechanisms illustrated in Fig. 2. Figure 2(a) shows the stripe, *pqrs*, before the edges relax the stress. In mechanism 1, the edges of the layer move outwards and in so doing, drag the lattice planes of the substrate along with them as shown in Fig. 2(b). This process relaxes stress in the layer and at the same time induces stress in the substrate.[2] In mechanism 2 [illustrated in Fig. 2(c)] the edges of the film again move outwards, but the substrate is not distorted.[5,8] We have made finite element calculations and found that in addition to the two mechanisms mentioned above, the edges cause stress relaxation by a third mechanism. In this mechanism shown in Fig. 2(d), the edges of the layer bend down and the central portion bulges up, making it curved, convex upwards.[14] Substrate planes also bend with a curvature which decreases as the distance from the interface increases. The details of the calculations will be published elsewhere.[13] The importance of this mechanism is also apparent in the experiments of Eaglesham *et al.*[15] and in recent finite element calculations of the stresses in islands.[16]

Since in both mechanisms 1 and 2 the edges of the compressed layer move out, it is important to understand the difference between the two mechanisms of stress relaxation. Lack of this understanding has caused much confusion in the existing literature.[3,6,8,11] In general the authors of earlier papers considered only one of these two mechanisms and assumed erroneously that the mechanism considered by them describes the total relaxation. In mechanism 1, the points p and r move together so that the line pr remains vertical. Relative motion of p and r is not permitted. In mechanism 2, the restriction that the points p and r must move by the same amounts is relaxed. However, in this mechanism acting alone the substrate distortion is neglected as if the substrate had infinite rigidity. No change of the dimensions of the interface is allowed during relaxation. Vertical displacement of any point in the interface is also not allowed. The point p moves outwards by a larger amount than the point r and thus relaxation in the upper parts of the layer is more than in the lower parts. Our finite element calculations show that in general all three mechanisms contribute to stress relaxation, but the third mechanism for stress relaxation at the middle of the stripe ($x'=l$) is important only for very narrow stripes with $l/h<2$, whereas the first and second mechanism are always important. Prior to our finite element calculations, the analytical models[3,6,11] or finite element calculations[5,8] of the stresses in the stripes took into account only either the first or the second mechanism.

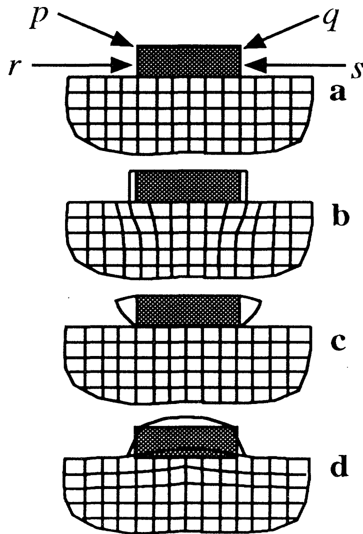

FIG. 2. Different mechanisms of strain relaxation are illustrated: (a) a pseudomorphic stripe *pqrs* before the edge induced relaxation is allowed to occur, (b) mechanism 1, (c) mechanism 2, and (d) mechanism 3.

Raman frequency has been measured only in the middle, $x=l$, of the surface layer of stripes.[10] Considerable simplification of the problem occurs if we confine our attention to this region. Our finite element calculations show that at $x'=l$ the stress is approximately independent of the substrate width $2l_s$ for $l/h \geq 3$. This is important because in Dietrich's experiments, $l=l_s$ and in the experiments on GaAs stripes on silicon,[5] $l_s \gg l$ (Ref. 5, and references given therein).

The Cartesian crystal coordinates are in the [100], [010], and [001] directions and are denoted by (x,y,z). The Cartesian stripe coordinates are in the $[\bar{1}\bar{1}0]$, $[\bar{1}10]$, and [001] directions and are denoted by (x',y',z') (see Fig. 1). The long dimension of the stripe is in the $[\bar{1}10]$ y' direction. The width is in the x' direction and height in the $z'=z$ direction. For convenience we will use primed symbols in the mesa coordinates (coordinate axes are defined in Fig. 1) instead of primed indices in the subscripts, i.e., we will use σ'_{yy} for $\sigma_{y'y'}$. Since the dimension of the stripe in the y' direction is large, ε'_{yy} remains constant at the value f_m determined by the misfit between the layer and the substrate. However stresses σ'_{xx} and σ'_{yy} are coupled together by Poisson's ratio and both vary with width due to relaxation at the edges of the stripe. The actual stress in the middle of the stripes is generally biaxial, i.e., the two orthogonal components σ'_{xx} and σ'_{yy} are not equal to each other. Relaxation of stress due to mechanism 1 in a *semi-infinite* stripe is given by[2]

$$\sigma'_{xx}(x)=\sigma_0-r'_{xx}(x)\ , \tag{1}$$

where

$$r'_{xx}(x)=\frac{2h}{K_{\mathrm{Hu}}\pi}\int_0^\infty \frac{\partial\sigma_{(f,xx)}(u)}{\partial u}\frac{du}{x-u}\ , \tag{2}$$

is the stress relaxation in a semi-infinite stripe (i.e., with one edge) and

$$K_{\mathrm{Hu}}=\frac{E_s(1-\nu_f^2)}{E_f(1-\nu_s^2)} \tag{3}$$

is a constant which depends on Young's modulus E and Poisson's ratio ν. The subscripts f and s denote the stripe and the substrate, respectively. $\sigma'_{xx}(x)$ has been calculated by Hu[2] for the semi-infinite layer. Fischer and Richter[6] used the principle of superposition to convert Hu's solution into that applicable to a stripe of finite width. However this procedure is not correct because the result does not satisfy the boundary condition that σ'_{xx} at the edges must be zero. We have solved Hu's equation numerically for a finite stripe, i.e., by evaluating numerically the integral in Eq. (2) between the finite limits 0 and $2l$. Since we will use these results for interpreting experiments on GeSi layers (with small Ge concentration) we have used $K_{\mathrm{Hu}}=1$. Values of relaxation due to mechanism 1, obtained in this manner, are plotted as the dashed curve in Fig. 3. Complete distributions of stresses for several widths of the stripes and their comparison with analytical solutions are given in Ref. 17.

The stress relaxation due to mechanism 2 has been calculated by Sakai, Kawasaki, and Wada[5] (see also Ref. 13 where an error in the original work has been corrected) and Van Mieghem *et al.*[8] using a finite element method. The strain relaxation due to this mechanism is shown by the long-short-dashed curve in Fig. 3. In linear elasticity theory relaxations due to different mechanisms can be added to obtain the final relaxations. Since mechanism 3 is not important for $l/h>3$, the total relaxation is obtained by adding the relaxations due to the first two mechanisms and is shown by the solid curve. For $l/h>3$, this curve agrees with our finite element calculations in which all the three mechanisms of stress relaxation have been included.[13] Since in earlier calculations only one of the first two mechanisms was used, they all underestimate the true relaxation.

The curves in Fig. 3 show many interesting features. For $l/h>50$, none of the relaxation mechanisms produces appreciable relaxation in the middle of the layer, the stress is the same as in an infinitely large layer to a good approximation. As l/h decreases stress relaxation increases and the relaxation due to substrate distortion (mechanism 1) increases more rapidly than that due to mechanism 2. Though relaxation due to mechanism 1 continues to be larger for $l/h>2$, the relaxation due to mechanism 2 is quite large and is not negligible. It is 30% of the relaxation due to mechanism 1 for $l/h=10$, increases rapidly as l/h decreases and becomes equal to that due to mechanism 1 for $l/h=2$. For $l/h<2$, relaxation due to mechanism 2 dominates over that caused by mechanism 1. As already mentioned mechanism 3 also becomes important in this regime.

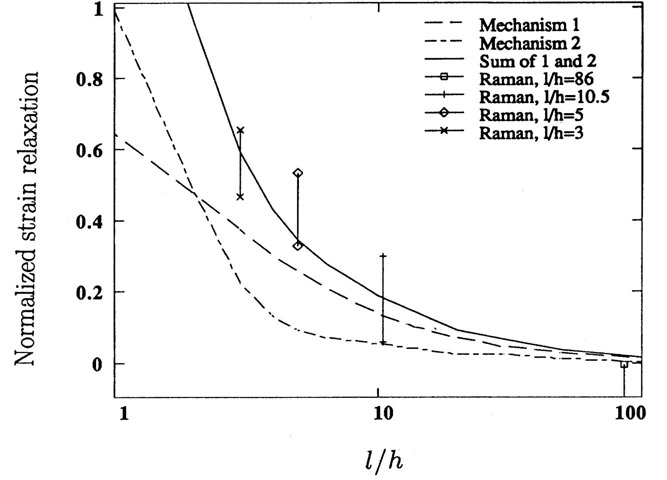

FIG. 3. Stress relaxation in the middle ($x=l$) of a stripe as a function of l/h. The dashed curve shows the relaxation due to substrate distortion (mechanism 1), the long-short-dashed curve gives relaxation without substrate distortion (mechanism 2), and the solid curve is the total relaxation obtained by adding these two relaxations. Relaxation due to mechanism 3 is not important for $l/h>3$. Symbols connected with error bars are the experimental values of stress relaxation obtained from Raman measurements.

III. SHIFT OF RAMAN FREQUENCY BY A COMBINATION OF UNIAXIAL AND BIAXIAL STRESSES

Dietrich *et al.*[10] have made accurate measurements of the shift $\Delta\omega_3$ of the Raman longitudinal optical (LO) mode due to stresses in the middle of the top layer of narrow $Ge_{0.14}Si_{0.86}$ stripes grown on patterned Si (100) substrates. The stripes were grown with their long dimension in the [110] direction. Measured values of $\Delta\omega_3$ for different widths $2l$ of the stripes were reported, but since an explicit relation between the stresses and Raman shifts was not known, values of stress and strain were not determined. We establish the required relation in this section.

In the presence of a biaxial or uniaxial stress, the triply degenerate phonon frequency ω_0 splits and the three components are shifted from ω_0 by amounts equal to $\Delta\omega_i$ where i takes values from 1 to 3. The relation between crystal strain components ε_{ij} (i and j take the values x, y, and z when used with the strain or stress components and 1, 2, and 3 when used with the elastic constants or with the shift $\Delta\omega$) and shifts $\Delta\omega_i$ is determined by the solution of the following secular equation derived by Anastassakis:[18]

$$\begin{vmatrix} \tilde{K}_{11}\varepsilon_{xx}+\tilde{K}_{12}(\varepsilon_{yy}+\varepsilon_{zz})-\lambda & 2\tilde{K}_{44}\varepsilon_{xy} & 2\tilde{K}_{44}\varepsilon_{xz} \\ 2\tilde{K}_{44}\varepsilon_{yx} & \tilde{K}_{11}\varepsilon_{yy}+\tilde{K}_{12}(\varepsilon_{zz}+\varepsilon_{xx})-\lambda & 2\tilde{K}_{44}\varepsilon_{yz} \\ 2\tilde{K}_{44}\varepsilon_{zx} & 2\tilde{K}_{44}\varepsilon_{zy} & \tilde{K}_{11}\varepsilon_{zz}+\tilde{K}_{12}(\varepsilon_{xx}+\varepsilon_{yy})-\lambda \end{vmatrix}=0 . \tag{4}$$

Here $\tilde{K}_{11}$, $\tilde{K}_{12}$, and $\tilde{K}_{44}$ are the phonon deformation potentials DP's,

$$\lambda_i = \frac{2}{\omega_0}\Delta\omega_i \tag{5}$$

and ω_0 is the Raman frequency of the bulk material. Two sets of values of DP's measured by Anastassakis[18] and Chandrasekhar, Renucci, and Cardona[19] are available and are given in Table I. To solve Eq. (4) we need the values of the strain components ε_{ij} in the crystal coordinates. We first calculate the strain and stress components in the stripe coordinates and then transform them into the crystal coordinates.

In a cubic crystal there are six independent strain components and six independent stress components related to each other by Hooke's law,

$$\sigma'_{ij} = \sum_{kl} c'_{ijkl}\varepsilon'_{kl} \ . \tag{6}$$

In our case the middle top surface of the Ge_XSi_{1-X} stripe is characterized by four known strain components and one known stress component. The strain components are

$$\varepsilon'_{yy} = f_m(X) = -X\frac{a_{Ge}-a_{Si}}{a_{Si}} \ , \tag{7}$$

and $\varepsilon'_{ij}=0$ for $i \neq j$. The stress component $\sigma'_{zz}=0$ because of the free surface boundary condition. This allows us to solve the Hooke's equation and determine all the stress and strain components in terms of one parameter σ'_{xx}. We assume $\sigma'_{xx}=\alpha\sigma_0$ where

$$\sigma_0 = f_m s = f_m\left[C_{11}+C_{12}-2\frac{C_{12}^2}{C_{11}}\right] \tag{8}$$

is the stress in an infinitely wide stripe. The constant α depends upon the dimensions of the stripe and it is as yet unknown. It corresponds to a pure uniaxial stress when $\alpha=0$ and *bisotropic* stress[20] (i.e., biaxial stress with σ'_{xx} equal to σ'_{yy}) when $\alpha=1$. We can now solve Hooke's equation and obtain all the stress and strain components in the stripe coordinates in terms of α. The elastic constants of GeSi in the crystal coordinates are obtained by linear interpolation between the elastic constants of Ge and Si given in Ref. 21. These elastic constants are converted into stripe coordinates as described in the Appendix at the end of the paper. The strain tensor is found to be

$$\{\varepsilon'\} = f_m\begin{bmatrix} \dfrac{s\alpha C_{11}-C_{11}(C_{12}-H/2)+C_{12}^2}{C_{11}(C_{11}+H/2)-C_{12}^2} & 0 & 0 \\ 0 & 1 & 0 \\ 0 & 0 & -\dfrac{s\alpha C_{12}+2C_{12}C_{44}}{C_{11}(C_{11}+H/2)-C_{12}^2} \end{bmatrix} , \tag{9}$$

TABLE I. Values of phonon deformation potentials and Raman frequency in bulk Si and Ge.

Material	ω_0 (cm^{-1})	$\tilde{K}_{11}$	$\tilde{K}_{12}$	$\tilde{K}_{44}$	T (K)	Refs.
Si	521	−1.85	−2.3	−0.7	110	18
Ge	300	−1.45	−1.95	−1.1	300	18
Si	521	−1.47	−1.95	−0.61	RT	19
Ge	300	−1.07	−1.6	−1.01		22

TABLE II. Calculated shifts $\Delta\omega_i$, $i=1,2,3$ in Raman frequency of GeSi strained layers (with respect to unstrained alloy) and different values of $\alpha=\sigma'_{xx}/\sigma_0$. Values calculated using deformation potentials of Anastassakis (Ref. 18) as well as of Chandrasekhar *et al.* (Ref. 19) are given.

	Using $\tilde{K}_{ij}$ of Ref. 18			Using $\tilde{K}_{ij}$ of Ref. 19		
α	$\Delta\omega_1$ (cm^{-1})	$\Delta\omega_2$ (cm^{-1})	$\Delta\omega_3$ (cm^{-1})	$\Delta\omega_1$ (cm^{-1})	$\Delta\omega_2$ (cm^{-1})	$\Delta\omega_3$ (cm^{-1})
0	2.84	0.44	2.21	2.37	0.25	1.92
0.1	2.91	0.74	2.46	2.41	0.51	2.14
0.2	2.97	1.05	2.71	2.45	0.76	2.36
0.3	3.03	1.35	2.96	2.50	1.01	2.57
0.4	3.10	1.65	3.21	2.54	1.27	2.79
0.5	3.16	1.96	3.45	2.58	1.52	3.00
0.6	3.23	2.26	3.70	2.62	1.77	3.22
0.7	3.29	2.57	3.95	2.66	2.03	3.44
0.8	3.35	2.87	4.20	2.70	2.28	3.65
0.9	3.42	3.18	4.45	2.75	2.53	3.87
1.0	3.48	3.48	4.70	2.79	2.79	4.08

where

$$H = 2C_{44} + C_{12} - C_{11} . \tag{10}$$

Similarly the stress tensor is given by

$$\{\sigma'\} = \begin{bmatrix} \alpha\sigma_0 & 0 & 0 \\ 0 & C'_{12}\varepsilon'_{xx} + C'_{11}\varepsilon'_{yy} + C'_{13}\varepsilon'_{zz} & 0 \\ 0 & 0 & 0 \end{bmatrix} . \tag{11}$$

The strain components are now transformed to the crystal coordinates (see the Appendix) to give

$$\{\varepsilon\} = \begin{bmatrix} \frac{1}{2}(\varepsilon'_{xx} + \varepsilon'_{yy}) & \frac{1}{2}(\varepsilon'_{xx} - \varepsilon'_{yy}) & 0 \\ \frac{1}{2}(\varepsilon'_{xx} - \varepsilon'_{yy}) & \frac{1}{2}(\varepsilon'_{xx} + \varepsilon'_{yy}) & 0 \\ 0 & 0 & \varepsilon'_{zz} \end{bmatrix} . \tag{12}$$

Using the strain components in the crystal coordinates given in Eq. (12), we solve the secular equation (4) and obtain

$$\lambda_{1,2} = \tilde{K}_{11}\varepsilon_{xx} + \tilde{K}_{12}(\varepsilon_{zz} + \varepsilon_{xx}) \mp 2\tilde{K}_{44}\varepsilon_{xy} , \tag{13}$$

$$\lambda_3 = \tilde{K}_{11}\varepsilon_{zz} + 2\tilde{K}_{12}\varepsilon_{xx} . \tag{14}$$

Here $\Delta\omega_i$ are the strain induced frequency shifts, ε_{ij} are the strain components in the crystal coordinates and λ_i is defined in Eq. (5).

Using the values of ε_{ij} given in Eq. (12) [with the value of ε'_{yy} given by Eq. (7) for $x = 0.14$] in Eqs. (13) and (14), and values of α in the range 0 to 1, we obtain the values of Raman shifts $\Delta\omega_i$ given in Table II. Only $\Delta\omega_3$ is observed in the back scattering geometry used in Dietrich's experiments. The calculated values of $\Delta\omega_3$ are shown by symbols in Fig. 4. We have fitted numerically the following equations with the values of $\alpha\sigma'_{xx}/\sigma_0$ shown in Fig. 4:

$$\sigma'_{xx}/\sigma_0 = 0.463\Delta\omega_3 - 0.890 \tag{15}$$

using Chandrasekhar's DP's (Ref. 19) and

$$\sigma'_{xx}/\sigma_0 = 0.4023\Delta\omega_3 - 0.890 \tag{16}$$

using Anastassiki's DP's.[18] The frequency $\Delta\omega_3$ in Eqs. (15) and (16) is in cm^{-1}. Solid curves in Fig. 4 show the plots of these equations. Equations (15) and (16) are the key results of this section. We will use these equations and Fig. 4 to determine σ'_{xx} using Dietrich's experimental results in Sec. IV.

Having determined α for a given stripe, all strain and stress components can be easily calculated using Eqs. (9) and (11).

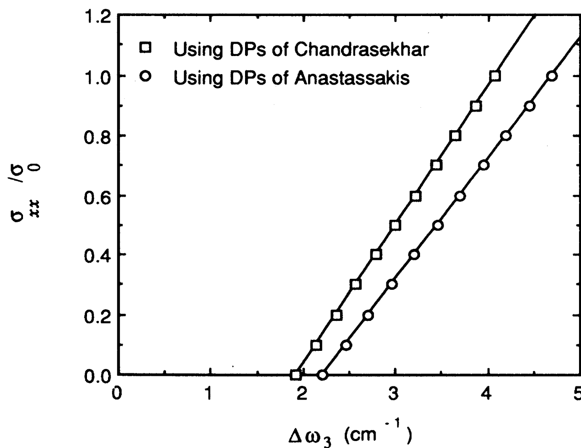

FIG. 4. Calculated values of σ'_{xx}/σ_0 for different values of Raman shifts $\Delta\omega_3$ are shown by symbols. Shifts calculated using two sets of values of phonon deformation potentials (DP's) measured by Chandrasekhar *et al.* (Ref. 19) (symbols, □□) and Anastassakis (Ref. 18) (symbols, ○○) are used. Curves are the plots of Eqs. (15) and (16) which are numerical fits to the data.

IV. EXPERIMENTAL VALUES OF STRESS RELAXATION: COMPARISON OF EXPERIMENTAL AND THEORETICAL RESULTS

In the experiments of Dietrich *et al.*,[10] 0.096-μm-thick $Ge_{0.14}Si_{0.86}$ stripes of different widths were grown on Si mesa stripes formed by patterning a (100) Si substrate by KOH anisotropic etch. Raman shifts $\Delta\omega_3$ were measured at midline on top of the stripes, in the valleys and outside the patterned region. The shifts in valleys and outside the patterned regions agreed with the values calculated for the bisotropic stress. The concentration of misfit dislocations in the stripes was measured using transmission electron microscopy and was found to be negligible. The observed shifts in the stripes are shown in Table III. Values of thickness and widths are also shown. Values of the normalized stress $\alpha = \sigma'_{xx}/\sigma_0$ for the observed shifts for each value of $1/h$ are read from Fig. 4 or calculated using Eqs. (15) and (16). We get two values of stress (and stress relaxation $1 - \sigma_{xx}$) for each sample, corresponding to the two values of the DP's. The values of stress relaxation for each sample are shown, joined by an "error bar," in Fig. 3. It is seen that the theoretical curve passes in between the two sets of experimental values except for the largest width. Thus experimental values agree with the calculated values within the uncertainty in the values of the DP's. The value of σ'_{xx}/σ_0 for the widest stripe

TABLE III. Observed shifts of Raman frequency in 0.096-μm-thick $Ge_{0.14}Si_{0.86}$ stripes of different widths (Ref. 10). Note that the frequency shifts given in Ref. 10 are with respect to Si frequency. We have obtained the shifts with respect to unstrained $Ge_{0.14}Si_{0.86}$ alloy by subtracting them from the alloy shift of 9.55 cm^{-1}.

$2l$ (μm)	l/h	$\Delta\omega_3$ (cm^{-1})
17.2	86	4.71
2.1	10.5	3.96
1.0	5.0	3.38
0.6	3.0	3.08

based on one of the DP's is more than unity; an impossible result. Since the Raman measurements and stress calculation for this stripe are the most reliable, it is clear that more reliable values of DP's are required. We have also estimated the correction necessary due to the finite width (about 0.8 μm) of the laser beam used to measure the Raman shift.[10] The laser beam "sees" not only the line in the middle of the stripe but areas adjacent to it, up to 0.4 μm away on each side. Using our finite element results, we estimated approximately the average stress over the width of the laser beam. The correction, the difference between the average stress and the stress at the middle, is practically zero for the stripe with $l/h=86$ and is about 10% for the narrowest stripe with $1/h=3$. The experimental points move downwards due to this correction. This correction does not change significantly the agreement between the calculated and experimental values of the relaxation.

Before concluding this section we must point out that the method described in this paper is general and can be used for stripes of any cubic semiconductor, irrespective of whether the strain is due to a difference in thermal expansion coefficients or due to lattice mismatch. The only important input from the experiment is the strain ε'_{yy} defined by Eq. (7). In the case of thermal strain, ε'_{yy} is determined by the difference in the thermal expansion coefficients of the stripe and the substrate and the temperature from which the heterostructure is cooled.

V. SUMMARY OF IMPORTANT RESULTS AND CONCLUDING REMARKS

We have calculated the stress in the middle of a narrow stripe (for $1/h>3$) including the effect of the two relaxation mechanisms which are relevant for these dimensions. For smaller values of this ratio, calculation of stress becomes more complicated and it is necessary to use finite element calculations including all three mechanisms. However, to date no experiments have been performed on such narrow stripes. Using existing values of phonon DP's, we have calculated shifts in Raman frequency due to any arbitrary relative values of stresses in the two inplane perpendicular directions of the stripe. This allows us to determine experimentally the stress values in the stripes using observed shifts in Raman frequency. The values of DP's determined by two different investigators differ significantly. Theoretical values of stress lie in between those determined from Raman experiments using the two sets of DP's. It is pointed out that improved values of DP's are required. We have also shown that the method developed in this paper is quite general and can be used for stripes of any cubic semiconductor and for thermal as well as lattice mismatch strains.

APPENDIX: TRANSFORMATION OF ELASTIC CONSTANTS TO STRIPE COORDINATES AND STRAINS TO CRYSTAL COORDINATES

In the stripe coordinates the z' axis has fourfold symmetry and the x' and y' axes both have twofold symmetry. Accordingly the matrix of elastic constants in the stripe coordinates has the following form[23] in the 6×6 representation:

$$\{C'\}=\begin{bmatrix} C'_{11} & C'_{12} & C'_{13} & 0 & 0 & 0 \\ C'_{12} & C'_{11} & C'_{13} & 0 & 0 & 0 \\ C'_{13} & C'_{13} & C'_{33} & 0 & 0 & 0 \\ 0 & 0 & 0 & C'_{44} & 0 & 0 \\ 0 & 0 & 0 & 0 & C'_{44} & 0 \\ 0 & 0 & 0 & 0 & 0 & C'_{66} \end{bmatrix} . \tag{A1}$$

Here the subscripts m and n of C'_{mn} have their conventional relationship to the generalized elastic constants C'_{ijkl}.

When the crystal axes are cubic (as is the case here) the matrix elements in Eq. (A1) can be calculated using the expression (see Ref. 21, p. 435)

$$C'_{ijkl}=C_{ijkl}-H\left[\sum_{n=1}^{3} T_{in}T_{jn}T_{kn}T_{ln}-\delta_{ij}\delta_{kl}\delta_{ik}\right] . \tag{A2}$$

In this expression C_{ijkl} are the elastic constants in the crystal axes, H is the anisotropy parameter defined in Eq. (10), and T_{ij} are the matrix elements in the matrix that transforms the axes from the crystal system to the stripe system. In the special case considered here, the transformation is a rotation of 45° about the z axis and the matrix is (Ref. 21, p. 4)

$$\{T\}=\begin{bmatrix} \frac{1}{\sqrt{2}} & \frac{1}{\sqrt{2}} & 0 \\ -\frac{1}{\sqrt{2}} & \frac{1}{\sqrt{2}} & 0 \\ 0 & 0 & 1 \end{bmatrix} . \tag{A3}$$

Substitution in Eq. (A2) yields the following relationship between C'_{mn} and C_{mn}:

$$\begin{aligned} C'_{11}&=C_{11}+\tfrac{1}{2}H \\ C'_{33}&=C_{11} \\ C'_{12}&=C_{12}-\tfrac{1}{2}H \\ C'_{13}&=C_{12} \\ C'_{44}&=C_{44} \\ C'_{66}&=C_{44}-\tfrac{1}{2}H . \end{aligned} \tag{A4}$$

Strains in the stripe coordinates are transformed to strains in the crystal coordinates using (Ref. 21, p. 39)

$$\varepsilon_{ij}=\sum_{l}\sum_{m} T_{li}T_{mj}\varepsilon'_{lm} . \tag{A5}$$

In the present case this is evaluated as

$$\{\varepsilon\}=\begin{bmatrix} \frac{1}{2}(\varepsilon'_{xx}+\varepsilon'_{yy})-\varepsilon'_{xy} & \frac{1}{2}(\varepsilon'_{xx}-\varepsilon'_{yy}) & \frac{1}{\sqrt{2}}(\varepsilon'_{xz}-\varepsilon'_{yz}) \\ \frac{1}{2}(\varepsilon'_{xx}-\varepsilon'_{yy}) & \frac{1}{2}(\varepsilon'_{xx}+\varepsilon'_{yy})+\varepsilon'_{xy} & \frac{1}{\sqrt{2}}(\varepsilon'_{xz}+\varepsilon'_{yz}) \\ \frac{1}{\sqrt{2}}(\varepsilon'_{xz}-\varepsilon'_{yz}) & \frac{1}{\sqrt{2}}(\varepsilon'_{xz}+\varepsilon'_{yz}) & \varepsilon'_{zz} \end{bmatrix} . \quad \text{(A6)}$$

---

*Present address: Interuniversity Micro-electronics Center, Kapeldreef 75, 3001 Leuven, Belgium.

[1]S. C. Jain, *Germanium-Silicon Strained Films and Heterostructures* (Academic, Boston, 1994).

[2]S. M. Hu, J. Appl. Phys. **50**, 4661 (1979).

[3]S. Luryi and E. Suhir, Appl. Phys. Lett. **49**, 140 (1986).

[4]E. Suhir, Mater. Res. Symp. Proc. **91**, 73 (1987).

[5]S. Sakai, K. Kawasaki, and N. Wada, Jpn. J. Appl. Phys. **29**, L853 (1990).

[6]A. Fischer and H. Richter, J. Appl. Phys. **75**, 657 (1994).

[7]G. P. Cherepanov, J. Appl. Phys. **75**, 844 (1994).

[8]P. Van Mieghem, S. C. Jain, J. Nijs, and R. Van Overstraeten, J. Appl. Phys. **75**, 666 (1994).

[9]W. C. Tang, H. J. Rosen, S. Guha, and A. Madhukar, Appl. Phys. Lett. **58**, 1644-6 (1991).

[10]B. Dietrich, E. Bugiel, H. J. Osten, and P. Zaumseil, J. Appl. Phys. **74**, 7223 (1993).

[11]L. Vescan, T. Stoica, C. Dieker, and H. Lüth, Mater. Res. Soc. Symp. Proc. **298**, 45 (1993).

[12]M. Grundmann, J. Christen, F. Heinrichsdorff, A. Krost, and D. Bimberg, J. Electronic Mater. **23**, 201 (1994).

[13]A. H. Harker, K. Pinardi, A. Atkinson, and S. C. Jain, Philos. Mag. A **71**, 871 (1995).

[14]If the stripe is under tensile stress, e.g., GaAs/Si, its edges will bend up and the central portion will be downwards, making it concave.

[15]D. J. Eaglesham and M. Cerullo, Phys. Rev. Lett. **64**, 1943 (1990).

[16]S. Christiansen, M. Albrecht, S. Strunk, and H. J. Maier, Appl. Phys. Lett. **64**, 3617 (1994).

[17]A. Atkinson, T. Johnson, A. H. Harker, and S. C. Jain (unpublished).

[18]E. Anastassakis, *Proceedings of the Sat. Symposium on ESSDERC 89 Berlin* (The Electrochemical Society, New York, 1989), Vol. 90-11, pp. 298–326.

[19]M. Chandrasekhar, J. B. Renucci, and M. Cardona, Phys. Rev. B **17**, 1623 (1978).

[20]E. Anastassakis, in *Light Scattering in Semiconductor Structures and Superlattices*, edited by D. J. Lockwood and J. F. Young, *NATO Advanced Study Institute Series B: Physics* (Plenum, New York, 1991), pp. 173–196.

[21]J. P. Hirth and J. Lothe, *Theory of Dislocations*, 2nd ed. (Wiley-Interscience, New York, 1982).

[22]Values of deformation potentials for Ge are not given in Ref. 19. The values given in the table are obtained by keeping the difference between the Ge and Si values the same as in the values reported in Ref. 18. Since Ge concentration is only 14%, the values of stress determined by us from Raman measurements are not sensitive to the deformation potential values for Ge.

[23]P. C. Waterman, Phys. Rev. **113**, 1240 (1959).